ISSN No:-2456-2165 https://doi.org/10.5281/zenodo.14608327

Study on Volumetric Efficiency, Heat Balance, and Air Fuel Ratio of Karanja Oil and Di-Tert Butyl Peroxide with Hydrogen as Fuel in a Diesel Engine

Sunil Mahto[1*]; Ashish Kumar Saha[2]
University Department of Chemistry, VBU, Hazaribagh, Jharkhand, India

Corresponding Author:- Sunil Mahto[1*]

Abstract:- Research into alternative fuels has been driven by the growing global energy demand, limited fossil fuel resources, exhaust pollutants, and the impact of climate change. Biodiesel, particularly its blends, is considered one of the most suitable and practical alternatives for diesel engines. This study was conducted using pure diesel and various blends of biodiesel derived from Karanja oil (BKO), di-tertiary butyl peroxide (DTBP), and hydrogen as a secondary fuel. The performance parameters observed include variations in heat in brake power (HBP), volumetric efficiency, air-fuel ratio, heat carried away by radiation (H Rad), heat carried away by exhaust gas (H Gas), and heat in jacket water (HJW). As the percentages of biodiesel (Karanja oil), DTBP, and hydrogen increased, the results showed that HBP increased by 19.15% due to hydrogen combustion in the cylinder. Volumetric efficiency decreased by 6.99% as hydrogen replaced some of the air. The air-fuel ratio decreased by 14.1% because hydrogen has a lower density compared to air. H Rad increased by 11.64% due to the rise in mean gas temperature, while H Gas and HJW decreased by 26.88% and 7.12%, respectively, due to the higher thermal conductivity resulting from the hydrogen-diesel fuel substitution.

Keywords:- *Diesel, Biodiesel of Karanja Oil, Di- Tertiary Butyl Peroxide, Hydrogen Fuel, and Performance.*

I. INTRODUCTION

The search for eco-friendly and sustainable fuels has increased due to population growth, the depletion of petrochemical resources, and the rising global demand for energy. Researchers have been focusing on finding alternative solutions to meet this growing energy need, particularly through the production and use of renewable oils. In this context, biodiesel and hydrogen fuel play a crucial role in addressing global fuel requirements [1]. For developing countries like India, producing biodiesel from non-edible oils that can be widely grown on wasteland is a more viable option [2]. Before large-scale adoption of biofuels, it is essential to assess their emission toxicity. Combustion in the engine cylinder produces exhaust gases, which can have adverse effects on health. Using Karanja oil biodiesel and diesel in engines enhances combustion efficiency due to the higher molecular oxygen content and cetane number of biodiesels. Lee et al. [3] examined the combustion properties of biodiesel blends made from soybean oil and rice bran oil in single-cylinder direct injection (CRDI) engines. These blends have been shown to reduce emissions of carbon monoxide (CO), hydrocarbons (HC), and particulate matter (PM) from the exhaust [4]. Common biodiesel blends made from oils such as sunflower, rapeseed, Jatropha, and Karanja are considered environmentally friendly alternatives to diesel. These fuels are non-toxic, renewable, clean-burning, biodegradable, and can be used directly or mixed with gasoline in diesel engines. However, certain compounds in Karanja oil, such as Karanjain and diketone panagmol, are toxic, which is why Karanja oil is not suitable for use as cooking oil. Baltacioglu et al. (2017) studied the use of Helianthus annus biodiesel blended with 10% hydrogen and HHO (Hydrogen-Hydroxy) fuel in diesel engines [5]. Their results showed that adding HHO improved engine performance compared to conventional diesel and pure hydrogen [6]. However, exhaust emissions increased with conventional diesel and pure hydrogen. Fossil fuel engine exhaust gases typically produce CO, NOX, and smoke, contributing to pollution [7]. Engine parameters, such as compression ratio and injection timing, significantly impact emissions and performance when using biodiesel blends. Many advanced technologies have been developed to address these issues, and newly designed engines may require modifications to optimize performance with biodiesel [8-9].

Biodiesel, especially methyl esters of fatty acids, is considered a suitable substitute for diesel. The use of vegetable oil and its derivatives as fuel in diesel engines has been extensively studied. Murugesan et al. (2009) [10] compared the engine parameters and thermophysical properties of biodiesel and diesel, with a focus on optimizing biodiesel production. Their study concluded that using biodiesel in compression ignition (CI) engines significantly reduces harmful emissions. Atadashi et al. [11] discussed biodiesel separation and quality enhancement technologies. Sharma and Murugan [12] also studied the use of Tyre Pyrolysis Oil (TPO) blends and Jatropha methyl ester (JME) biodiesel to assess diesel engine behavior.

In engines, the air-fuel ratio decreases as load increases, leading to higher fuel consumption. As the

ISSN No:-2456-2165 https://doi.org/10.5281/zenodo.14608327

biodiesel content in blends increases, the air-fuel ratio for diesel-waste cooking oil biodiesel blends becomes lower compared to pure diesel [13]. Dual-fuel engines, which have mixed combustion characteristics, require careful management of the air-fuel ratio, as it significantly impacts engine efficiency. However, the effects of the air-fuel ratio under different engine settings have not been thoroughly studied, though some researchers have considered it in their experimental designs [14].

In an engine, a fan and radiator are used to cool hot jacket water, which is then returned to the cooling system. At low loads, the jacket water temperature is lower, and preheating the oil may be necessary [15-17]. The maximum integral heat release values for Karanja and Jatropha biodiesel were similar under different load conditions, with their heat release behavior comparable to fossil diesel at higher loads [18]. The carbon and hydrogen contents in biodiesel molecules result in different stoichiometric air-fuel ratios, heating values, and adiabatic flame temperatures. The presence of oxygen in biodiesel also reduces soot formation, which decreases radiation heat transfer and increases reaction temperatures [19].

Blends of Karanja oil esterified biodiesel (B20 and B40) are an acceptable substitute for diesel fuel and help reduce air pollution by lowering brake power heat (HBP) [20]. To improve engine performance, this research aims to determine the volumetric efficiency of Pertamina biodiesel (D70J30) [21] blended fuel. Low heat rejection (LHR) engines, which reduce heat transfer between the cylinder liner and in-cylinder gas by insulating combustion elements, offer a promising solution. The LHR concept suppresses heat rejection to the coolant and recovers energy as useful work. This approach also reduces engine noise and improves fuel economy, while exhaust gases contain higher energy [22-25].

II. EXPERIMENTAL DETAILS

The experimental setup for the dual-fuel mode of a diesel engine (as shown in Figs. 1a and 1b) was based on a single-cylinder, four-stroke engine with a power output of 3.5 kW at 1500 rpm. The engine used is the Kirloskar TV1 model, which includes a specific compression ratio. It was connected to an eddy current-type dynamometer, which was used for loading the engine during the experiment. The experimental analysis utilized several instruments, including a digital indicator, a panel box, a fuel measuring device, a manometer, a fuel tank, and a digital temperature indicator. Data for engine performance analysis was collected using MS Excel and IC engine software. The hydrogen cylinder setup, which supplied hydrogen as the secondary fuel, included a pressure regulator, flame arrester, flashback arrester, and a rotameter with a one-way non-return valve, as detailed in Table 1 [26].

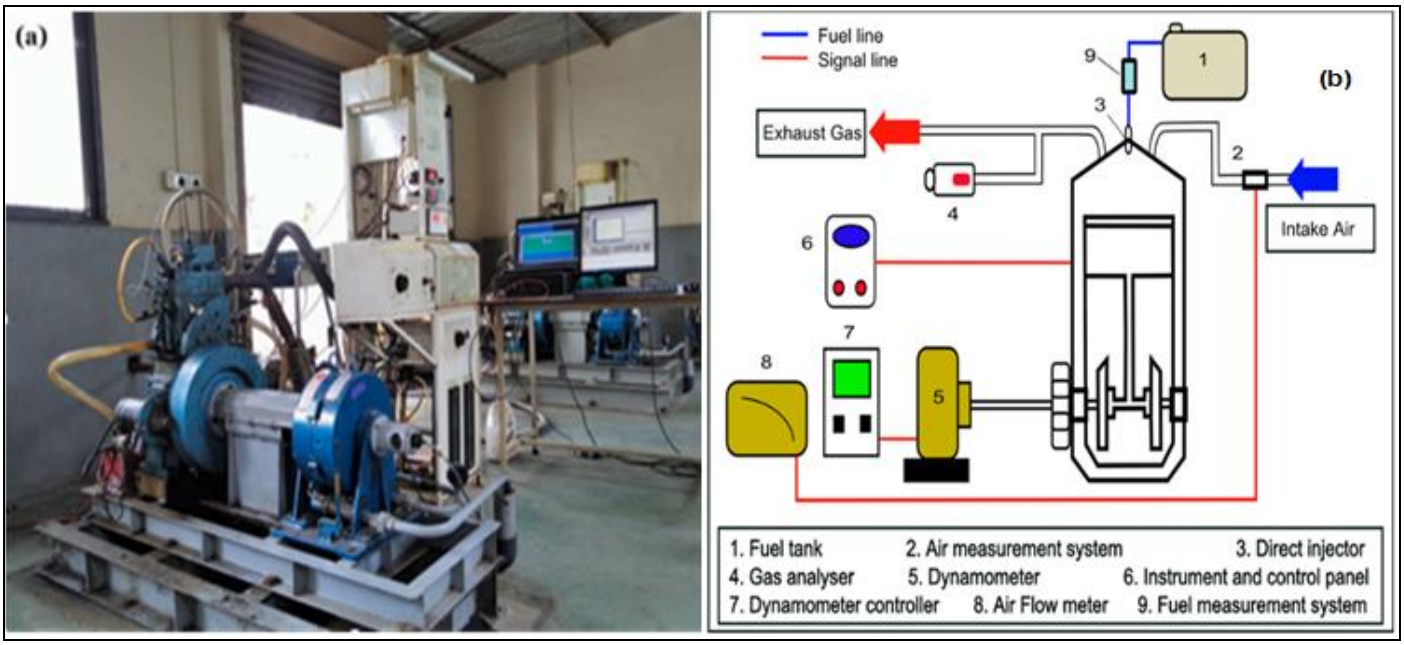

Fig 1 (a)- Experimental Photographic view. (b) - Experimental Set-up Schematic view

Table 1 Scientific Capacity of the Engine [26]

S. No.	Factors	Measurements	Units
1	Swept volume	661.45	cc
2	Rated speed	1500	RPM
3	Bore × Stroke	87.50×110	mm × mm
4	No. of cylinder	1	-
5	Engine type	Single cylinder four-strokes, CI engine, etc.,	-
6	Make and model	Model Kirloskar, TV1	-
7	Inlet temperature	300	K

ISSN No:-2456-2165 https://doi.org/10.5281/zenodo.14608327

8	Inlet pressure	1.03	bar
9	Rated power	3.5	KW
10	Injection timing BTC	19	^oC
11	Injection pressure	224.11	bar
12	Compression ratio	18	-

Table 2 The values of Performance Parameters with Different Load Conditions

D-80%+B-20%						
Load (%)	Volumetric efficiency (%)	Air-fuel ratio	HBP (%)	HJW (%)	H Gas (%)	H Rad (%)
2	28.95	0.4	0	82.13	72.65	0
18	28.39	0.65	0.75	80.71	43.85	11.81
36	27.82	0.85	0.49	79.1	32.87	18.07
53	27.82	1	0.39	79	27.94	23.07
69	27.63	1.29	0.38	78.67	21.34	23.6
D-79% + B-20% + A-1% + H-7%						
Load (%)	Volumetric efficiency (%)	Air-fuel ratio	HBP (%)	HJW (%)	H Gas (%)	H Rad (%)
2	28.95	0.45	0	82.29	64.58	0
18	28.76	0.7	0.81	81.77	41.25	10.95
36	27.63	0.9	0.52	78.56	30.83	17.03
53	27.63	1.2	0.52	78.56	23.12	17.03
69	27.25	1.34	0.43	77.46	20.26	20.81
D-79% + B-20% + A-1% + H-11%						
Load (%)	Volumetric efficiency (%)	Air-fuel ratio	HBP (%)	HJW (%)	H Gas (%)	H Rad (%)
2	28.2	0.35	0	80.29	80.9	0
18	28.2	0.55	0.64	80.07	51.48	13.95
36	27.44	0.75	0.43	78.12	36.73	20.4
53	27.25	1.15	0.44	77.46	23.79	19.99
69	27.05	1.34	0.43	77.01	20.12	20.78
D-79% + B-20% + A-1% + H-16%						
Load (%)	Volumetric efficiency (%)	Air-fuel ratio	HBP (%)	HJW (%)	H Gas (%)	H Rad (%)
2	28.39	0.45	0	80.77	63.34	0
18	27.82	0.55	0.64	79.05	50.79	13.94
36	27.25	0.85	0.49	77.41	32.18	18.04
53	26.85	1.15	0.44	76.3	23.45	20
69	26.46	1.39	0.44	75.27	18.97	20.05
D-79% + B-20% + A-1% + H-20%						
Load (%)	Volumetric efficiency (%)	Air-fuel ratio	HBP (%)	HJW (%)	H Gas (%)	H Rad (%)
2	28.01	0.4	0	79.75	70.32	0
18	27.82	0.55	0.64	79.1	50.79	13.93
36	27.25	0.85	0.49	77.56	32.18	18
53	26.66	1.15	0.44	75.58	23.27	20.04
69	26.05	1.39	0.44	74.12	18.68	20.05
D-79% + B-20% + A-1% + H-25%						
Load (%)	Volumetric efficiency (%)	Air-fuel ratio	HBP (%)	HJW (%)	H Gas (%)	H Rad (%)
2	28.01	0.45	0	79.49	62.5	0
18	27.82	0.6	0.69	79.1	46.56	12.77
36	27.25	0.9	0.52	77.46	30.4	17.03
53	26.46	1.2	0.46	75.17	22.14	19.17
69	26.26	1.49	0.47	74.64	17.57	18.73

ISSN No:-2456-2165 https://doi.org/10.5281/zenodo.14608327

Table 3 The values of Performance Parameters with Different Load Conditions

D-70%+B-30%						
Load (%)	Volumetric efficiency (%)	Air-fuel ratio	HBP (%)	HJW (%)	H Gas (%)	H Rad (%)
2	29.49	0.45	0	83.78	65.8	0
18	28.76	0.7	0.81	81.71	41.25	10.98
36	28.39	0.9	0.52	80.55	31.67	17.1
53	28.2	1.2	0.46	80.18	23.6	19.2
69	27.63	1.25	0.36	78.46	22.2	24.61
D-67% + B-30% + A-3% + H-7%						
Load (%)	Volumetric efficiency (%)	Air-fuel ratio	HBP (%)	HJW (%)	H Gas (%)	H Rad (%)
2	28.76	0.5	0	81.55	57.75	0
18	27.82	0.6	0.69	79	46.56	12.82
36	27.05	0.85	0.59	76.86	31.95	15.07
53	26.85	1.2	0.52	76.35	22.47	17.06
69	26.66	1.39	0.44	75.83	19.12	20.1
D-67% + B-30% + A-3% + H-11%						
Load (%)	Volumetric efficiency (%)	Air-fuel ratio	HBP (%)	HJW (%)	H Gas (%)	H Rad (%)
2	27.82	0.35	0	78.9	79.82	0
18	27.82	0.6	0.69	79.05	46.56	12.81
36	27.05	0.9	0.52	76.81	30.18	17.09
53	26.85	1.2	0.46	76.35	22.47	19.2
69	26.46	1.29	0.41	75.42	20.43	21.6
D-67% + B-30% + A-3% + H-16%						
Load (%)	Volumetric efficiency (%)	Air-fuel ratio	HBP (%)	HJW (%)	H Gas (%)	H Rad (%)
2	27.63	0.35	0	78.56	79.27	0
18	27.63	0.6	0.69	78.51	46.24	12.81
36	27.05	0.9	0.52	76.86	30.18	17.08
53	26.26	1.15	0.44	74.6	22.92	20.05
69	26.05	1.39	0.44	74.02	18.68	20.13
D-67% + B-30% + A-3% + H-20%						
Load (%)	Volumetric efficiency (%)	Air-fuel ratio	HBP (%)	HJW (%)	H Gas (%)	H Rad (%)
2	27.44	0.4	0	78.01	68.88	0
18	27.25	0.55	0.64	77.36	49.74	13.98
36	26.66	0.8	0.46	75.78	33.45	19.2
53	26.26	1.15	0.44	74.6	22.92	20.05
69	25.85	1.39	0.44	73.44	18.54	20.13
D-67% + B-30% + A-3% + H-25%						
Load (%)	Volumetric efficiency (%)	Air-fuel ratio	HBP (%)	HJW (%)	H Gas (%)	H Rad (%)
2	27.44	0.35	0	78.07	78.72	0
18	27.44	0.55	0.64	77.96	50.09	13.97
36	27.05	0.9	0.52	76.81	30.18	17.09
53	26.26	1.2	0.46	74.6	21.97	19.21
69	25.85	1.34	0.43	73.39	19.22	20.88

Table 4 The values of Performance Parameters with Different Load Conditions

D-60%+B-40%						
Load (%)	Volumetric efficiency (%)	Air-fuel ratio	HBP (%)	HJW (%)	H Gas (%)	H Rad (%)
2	29.31	0.45	0	83.22	65.39	0
18	28.95	0.65	1.13	82.24	44.71	7.98
36	28.58	0.85	0.49	81.24	33.75	18.29
53	28.2	1.05	0.46	80.34	26.97	19.7
69	28.01	1.34	0.43	79.64	20.83	21.11
D-55% + B-40% + A-5% + H-7%						
Load (%)	Volumetric efficiency (%)	Air-fuel ratio	HBP (%)	HJW (%)	H Gas (%)	H Rad (%)
2	28.95	0.5	0	82.29	58.12	0
18	28.01	0.75	0.87	79.54	37.5	10.38
36	27.63	0.95	0.55	78.56	29.2	16.37
53	27.44	1.39	0.41	78.07	19.68	22.2
69	27.26	1.56	0.36	76.02	15.23	26.03

ISSN No:-2456-2165 https://doi.org/10.5281/zenodo.14608327

D-55% + B-40% + A-5% + H-11%						
Load (%)	Volumetric efficiency (%)	Air-fuel ratio	HBP (%)	HJW (%)	H Gas (%)	H Rad (%)
2	28.2	0.45	0	80.07	62.93	0
18	28.01	0.7	0.81	79.54	40.18	11.12
36	27.44	0.85	0.59	78.01	32.41	15.24
53	26.66	1.15	0.5	75.78	23.27	18.03
69	26.85	1.34	0.43	76.3	19.97	21.13
D-55% + B-40% + A-5% + H-16%						
Load (%)	Volumetric efficiency (%)	Air-fuel ratio	HBP (%)	HJW (%)	H Gas (%)	H Rad (%)
2	27.63	0.3	0	78.46	92.48	0
18	27.82	0.55	0.64	79.1	50.79	14.13
36	27.05	0.9	0.52	76.96	30.18	17.26
53	26.66	1.1	0.48	75.68	24.33	18.87
69	26.46	1.25	0.39	75.17	21.25	22.82
D-55% + B-40% + A-5% + H-20%						
Load (%)	Volumetric efficiency (%)	Air-fuel ratio	HBP (%)	HJW (%)	H Gas (%)	H Rad (%)
2	27.44	0.35	0	78.01	78.72	0
18	27.63	0.6	0.69	78.51	46.24	12.96
36	26.85	0.85	0.59	76.35	31.72	15.24
53	26.46	1.05	0.4	75.17	25.3	22.22
69	26.05	1.29	0.38	74.17	20.12	23.89
D-55% + B-40% + A-5% + H-25%						
Load (%)	Volumetric efficiency (%)	Air-fuel ratio	HBP (%)	HJW (%)	H Gas (%)	H Rad (%)
2	27.63	0.6	0	78.67	46.24	0
18	27.44	0.55	0.64	78.12	50.09	14.11
36	27.05	0.8	0.46	76.86	33.95	19.45
53	26.46	1.1	0.42	75.27	24.15	21.19
69	26.05	1.39	0.4	73.97	18.68	22.24

III. METHODS AND MATERIALS

➢ *Biodiesel Oxidation Chemistries:*

The detailed hydrogen reaction mechanism by Mahto et al. [26], along with the skeletal soot generation and oxidation kinetics, was integrated to create a biodiesel reaction mechanism designed for hydrogen-assisted biodiesel combustion chemistry. This mechanism is a tri-component system. In addition to the chemical reaction kinetics, the reaction mechanism of biodiesel involves the interaction between methyl decanoate (MD) and methyl-9-decanoate (M9D) with n-heptane.

Tao et al. analyzed 204 elementary reactions and 69 species in the reaction mechanisms of CO and computational fluid dynamics (CFD) applications, which are highly practical. Their study shows that acetylene (C2H2) reacts with hydrogen, leading to the formation of an aromatic ring. This soot formation mechanism is driven by a series of elementary reactions involving the Ai radical. The successive steps, including C2H2 addition and hydrogen abstraction (HACA mechanism), result in the formation of an aromatic chain. This chain then forms the phenyl Ai radical and the initial aromatic ring, which undergoes further reactions. The general reaction steps for the formation of larger aromatic rings are described as follows.

$$Ai + H \longrightarrow Ai^{*} + H_2 \quad (1)$$

$$Ai^{*} + C_2H_2 \longrightarrow Ai^{*}C_2H_2 \quad (2)$$

$$Ai^{*}C_2H_2 + H \longrightarrow Ai^{*}C_2H + H_2 \quad (3)$$

$$Ai^{*}C_2H + C_2H_2 \longrightarrow A_{i+1} \quad (4)$$

The radical corresponding to a higher ring is represented as A_{i+1}. A one-step transition from the aromatic ring to soot is proposed at a sufficiently high order. In this study, the formation of soot is described by equations (6) and (7), which also outline the oxidation mechanism of soot in the subsequent explanation [26]. Furthermore, for long-chain acetylene (A_2R_5), ace-naphthalene, and C_6H_2, soot growth occurs alongside the formation of higher-order rings during the "graphitization" process.

$$C_6H_2 \longrightarrow H_2 + 6C(S) \quad (5)$$

$$A_2R_5 \longrightarrow 4H_2 + 12C(S) \quad (6)$$

To make the simulation of 1 mole of n-heptane, using 0.5 mol of MD and 0.5 mol of M9D for pure biodiesel, more practical, a three-dimensional computational fluid dynamics simulation with 107 species and 443 elementary reactions was used. Additionally, ignition delay calculations and sensitivity analysis were carried out for pressures ranging from 1 to 100 atm and equivalence ratios from 0.5 to 2. The

ISSN No:-2456-2165 https://doi.org/10.5281/zenodo.14608327

ignition delay times of the developed reaction mechanism were compared to those of a detailed reaction mechanism, which includes 10,806 reactions and 3,299 species. It was found that the optimal initial temperatures for the reaction mechanism were between 700 and 1800 K, as reported.

Following this, a sensitivity analysis was conducted on the ignition delay time, which is highly sensitive and described by the reactions shown in equations 8-10. To improve ignition delay predictions, the activation energy (E) and pre-exponential factor (A) were used for these reactions, based on parametric modifications and testing conditions as outlined below.

$$MD + HO_2 \longrightarrow MD6J + H_2O_2 \quad 4.410E+02 \quad 1.764E+03 \quad (7)$$

$$MD + HO_2 \longrightarrow MD6J + H_2O_2 \quad 4.410E+02 \quad 1.764E+03 \quad (8)$$

$$MD9 \longrightarrow C_2H_4 + MD5J + C_3H_5 \quad 1.563E+15 \quad 6.250E+16 \quad (9)$$

➢ *To Study the Fission of Kinetic of Di-Tert-Butyl Peroxide*

Unlike pure diesel fuel, where DTBP participates in the combustion process, hydrogen is used as a secondary fuel in dual-fuel engines to reduce ignition delay. By incorporating DTBP, a batch computer-aided design (CAD) tool is used to simulate and model the reaction kinetics. In addition to serving as a radical source to initiate the reaction, the fission of the weak RO-OR bond at temperatures above 393 K causes DTBP to oxidize and dissociate into two RO radicals at the maximum temperature.

The reaction proceeds as follows: it produces two moles of oxide radicals in the form of acetone (propane-2-one), with the methyl radical acting as an intermediate product, alongside DTBP.

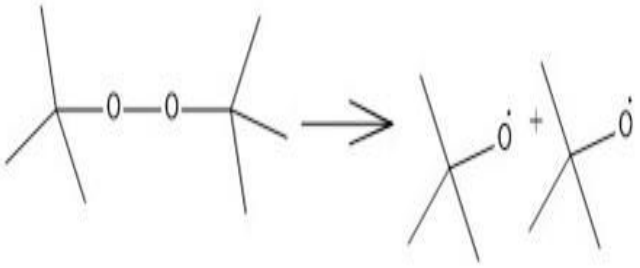

The formation of methyl radicals, and acetone by the rearrangement of unstable radicals.

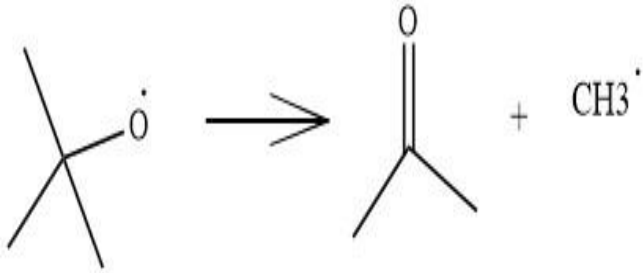

The reaction occurs in two steps. In the first step, DTBP undergoes fission, producing acetone at lower temperatures. At higher temperatures, acetone undergoes chain branching through ethane combustion, leading to the formation of a stable intermediate acetone. This intermediate remains nearly stable at 1100 K until the major reaction begins. Methyl radicals are produced during combustion. Due to the presence of DTBP, the initial temperature increase triggers a highly exothermic reaction for DTBP oxidation. The reaction mechanism of DTBP was further studied to reduce ignition delay. Additionally, DTBP interacts with diesel mixtures by fissioning through the base fuel, rapidly releasing heat.

To reduce ignition delay in diesel engines in a very short period, thermal fission is used by raising the temperature to support DTBP. As the temperature increases, the thermal fission of DTBP in diesel engines shortens the ignition delay. Moreover, when DTBP is added, it improves the cetane number and reduces emissions compared to standard diesel fuel.

DTBP acts as a substrate that undergoes photolytic decomposition. The rate of abstraction has activation energy of 11.7 kcal/mole, typically ignored. The first-order reaction for consistent decomposition results in a constant rate, with the initial outcome having a feasible effect. The following stoichiometric equations are presented in [27].

The rate constant and pressure having k1 = $10^{13} \rightarrow 10^{16} \times e^{(-34 \rightarrow -39 kcal/RT)}$ sec-1 and 0→600 mmHg in step 1 without any chain reaction. The reaction steps mentioned above consider two points.

$$t\text{-BuO} + Me \longrightarrow t\text{-BuOMe} \quad \text{Step 7}$$

$$t\text{-BuO}^{\cdot} + DTBP \xrightarrow{-H} t\text{-BuOH} + DTBP^{\cdot} \quad \text{Step 8}$$

$$DTBP \xrightarrow{-H} \text{(epoxide)} + t\text{-BuO}^{\cdot} \quad \text{Step 9}$$

➢ *A Decomposition Reaction of T-Butyl Methyl Ether is-*

$$DTBP \longrightarrow t\text{-BuOMe} + Me_2CO$$

Two-mole products were formed by 1 mole of DTBP in steps of reactions 8 and 9. Further, three-mole products through methyl radicals are observed.

$$DTBP \longrightarrow CH_4 + i\text{-BuO} + Me_2CO$$

A methyl radical treated with peroxy radical undergoes decomposition of t-amyl-t-butyl peroxide with the involvement of 10% by stoichiometry method.

ISSN No:-2456-2165 https://doi.org/10.5281/zenodo.14608327

The formation of 90% product in the exothermic reaction (39 kcal/mol) and enhancement in rate 1 to a greater extent by enhancing the preliminary pressure.

$$DTBP \longrightarrow 2Me_2CO + C_2H_6$$

At the maximum temperature, the diameter of the reaction vessel is influenced by the reactant pressure and thermal gradient, reaching its peak value. Under standard experimental conditions, an exothermic reaction occurs at 150°C and 7.5 atm, which are well within the acceptable limits.

The process for producing t-butanol involves a summary of the stoichiometry for analysis. The amount of isobutylene oxide generated is used to assess a chain of the thermostat (multi-contact) through a specific vessel. This results from an experimental multi-surface reaction in a typically spherical reaction vessel, which helps minimize temperature gradients. Finally, the experimental design aimed at resolving these conflicting factors is linked to the use of a reaction vessel.

IV. RESULTS AND DISCUSSION

The volumetric efficiency of the engine decreases as the proportion of Karanja oil biodiesel (BKO) increases from 20% to 40%, the additive concentration rises from 1% to 5%, and the hydrogen percentage as a secondary fuel increases from 7% to 25% in pure diesel, particularly under high load conditions. This decline in volumetric efficiency is likely due to the displacement of air by hydrogen, which has a lower density compared to air. As the percentages of BKO and hydrogen increase, the lower density of hydrogen reduces the amount of air inducted into the engine, leading to a decrease in volumetric efficiency. This effect becomes more significant with higher levels of hydrogen substitution, which appears to be the main reason for the observed reduction in volumetric efficiency at higher concentrations of hydrogen and biodiesel.

The air-fuel ratio increases with the addition of Karanja oil biodiesel (BKO) from 20% to 30%, the additive from 1% to 5%, and hydrogen from 7% to 25% in each diesel and BKO composition. However, with the addition of 40% BKO in pure diesel with the additive and hydrogen, the air-fuel ratio decreases under high-load conditions. This decrease is due to the lower density of hydrogen compared to air, which results in less air intake as hydrogen displaces air.

Regarding brake power (HBP), it increases with the addition of BKO from 20% to 30%, the additive from 1% to 5%, and hydrogen from 7% to 25% in each diesel and BKO composition at high-load conditions. This increase is attributed to the smoother combustion of hydrogen, which is in gaseous form inside the engine cylinder. However, at 40% BKO addition in pure diesel with the additive and hydrogen, HBP decreases at high-load conditions.

For heat in jacket water (HJW) and heat carried away by exhaust gas (H Gas), both decrease with the increasing percentage of BKO (20% to 40%), the additive (1% to 5%), and hydrogen (7% to 25%) as a secondary fuel in pure diesel at high-load conditions. This is because BKO and hydrogen have higher thermal conductivity compared to air in diesel operation, which reduces the heat transfer to jacket water and exhaust gases.

Heat carried away by radiation (H Rad) decreases with the addition of BKO from 20% to 30%, the additive from 1% to 5%, and hydrogen from 7% to 25% in each diesel and BKO composition. However, when 40% BKO is added to pure diesel with the additive and hydrogen, H Rad increases at high-load conditions. This increase is due to the higher mean gas temperature resulting from the substitution of diesel with hydrogen fuel, which increases the fraction of heat radiated at higher loads.

Figures 2-19 show the variations in volumetric efficiency, air-fuel ratio, heat in brake power (HBP), heat in jacket water (HJW), heat carried away by exhaust gas (H Gas), and heat carried away by radiation (H Rad) under different loads (from 2% to 69%) and various fuel compositions. The figures indicate a decrease in volumetric efficiency, HBP, HJW, and H Gas, and an increase in air-fuel ratio and H Rad as the load increases from 2% to 69%.

For the fuel composition (D-79% + B-20% + A-1% + H-7%), the decreases in volumetric efficiency, HJW, H Gas, and H Rad were 1.37%, 1.54%, 5.06%, and 11.8%, respectively, while the air-fuel ratio and HBP increased by 3.73% and 11.6%, respectively, at high-load conditions (Fig. 2). In the case of the fuel composition (D-79% + B-20% + A-1% + H-11%), the decreases in volumetric efficiency, HJW, H Gas, and H Rad were 2.09%, 2.11%, 5.71%, and 11.95%, respectively, while the air-fuel ratio and HBP increased by 3.87% and 11.6%, respectively (Fig. 3). Similarly, for the fuel composition (D-79% + B-20% + A-1% + H-16%), the decreases in volumetric efficiency, HJW, H Gas, and H Rad were 4.23%, 4.32%, 11.1%, and 15.04%, respectively, while the air-fuel ratio and HBP improved by 7.2% and 13.6%, respectively (Fig. 4). For the composition (D-79% + B-20% + A-1% + H-20%), the decreases in volumetric efficiency, HJW, H Gas, and H Rad were 5.71%, 5.78%, 12.46%, and 15.04%, respectively, and the air-fuel ratio and HBP increased by 7.2% and 13.6%, respectively (Fig. 5). Lastly, in the case of the fuel composition (D-79% + B-20% + A-1% + H-25%), the decreases in volumetric efficiency, HJW, H Gas, and H Rad were 4.95%, 5.12%, 17.67%, and 20.6%, respectively, while the air-fuel ratio and HBP increased by 13.4% and 19.15%, respectively (Fig. 6) (Table 2).

ISSN No:-2456-2165 https://doi.org/10.5281/zenodo.14608327

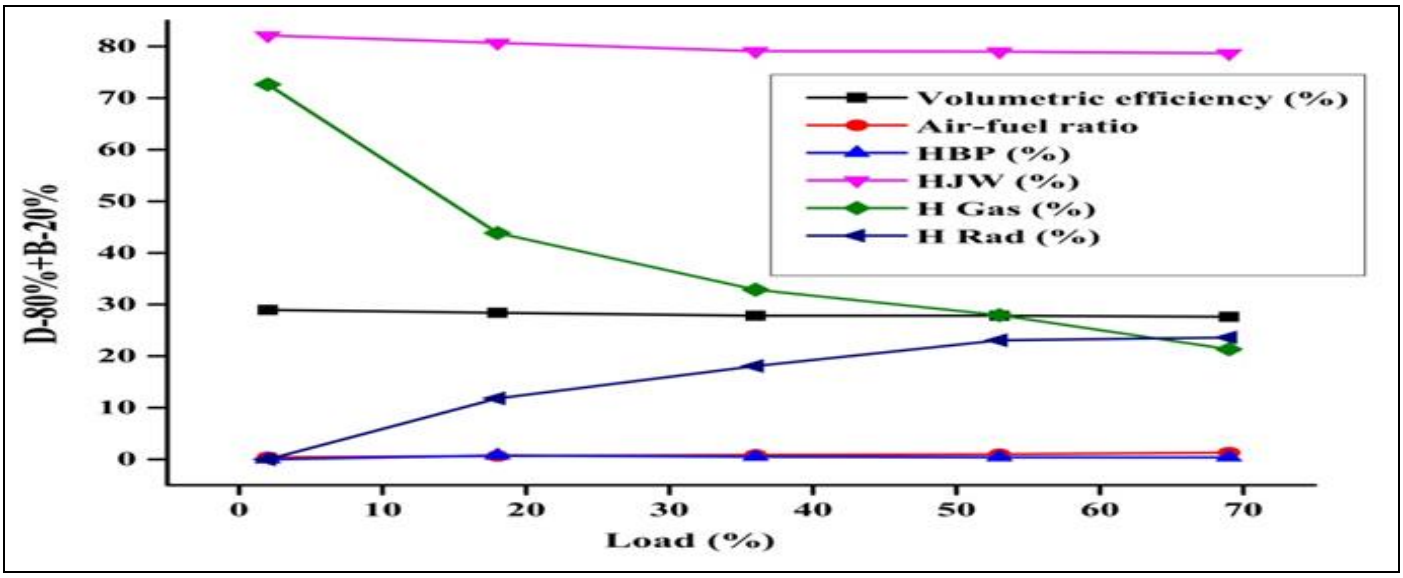

Fig 2 Variation of Compositions of Fuel Versus Loads Percentages.

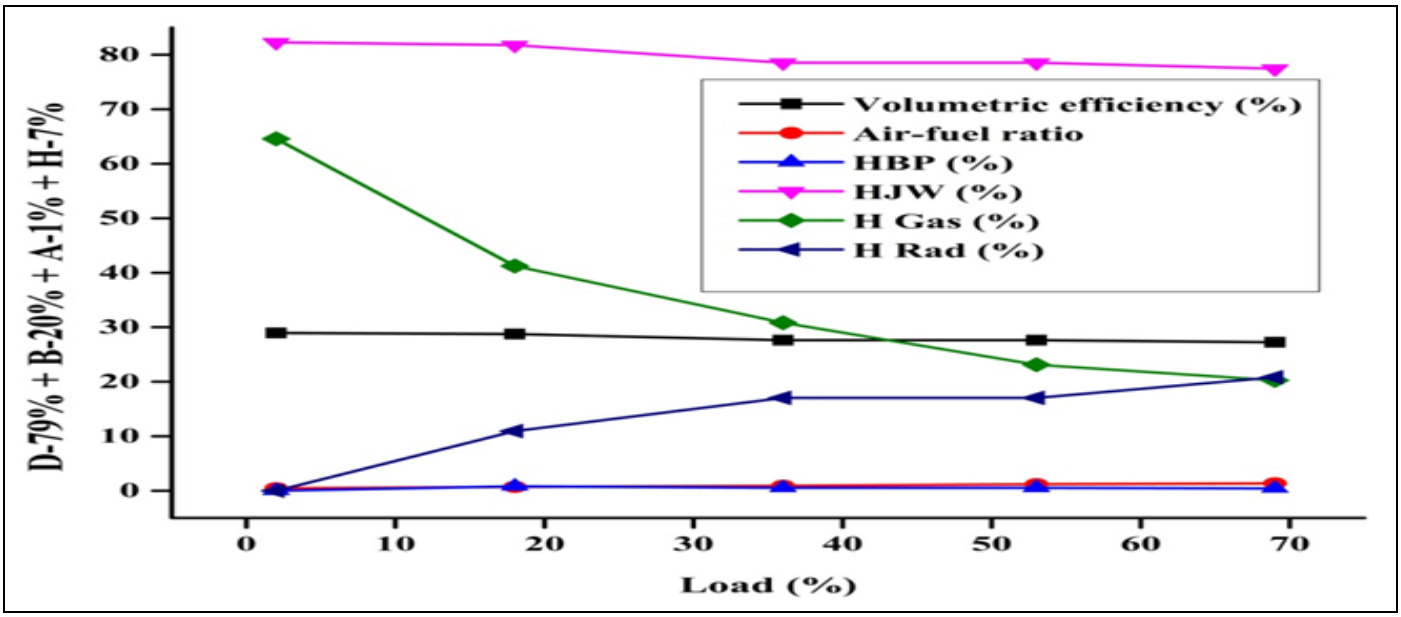

Fig 3 Variation of Compositions of Fuel Versus Loads Percentages.

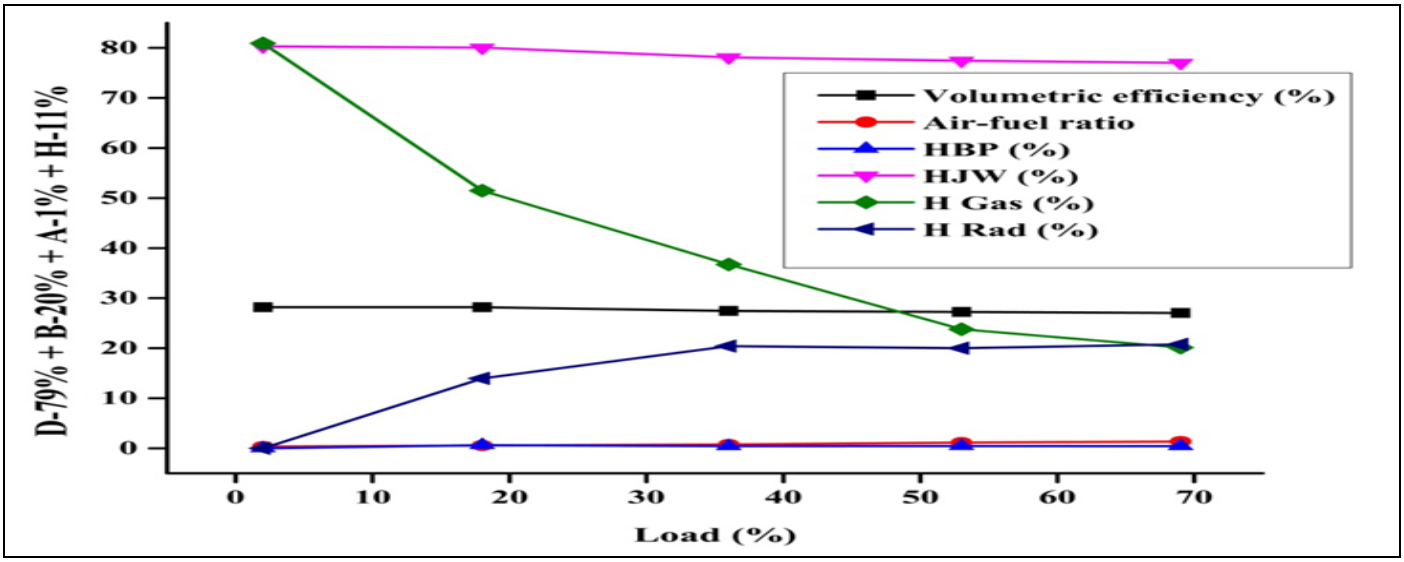

Fig 4 Variation of Compositions of Fuel Versus Loads Percentages.

ISSN No:-2456-2165 https://doi.org/10.5281/zenodo.14608327

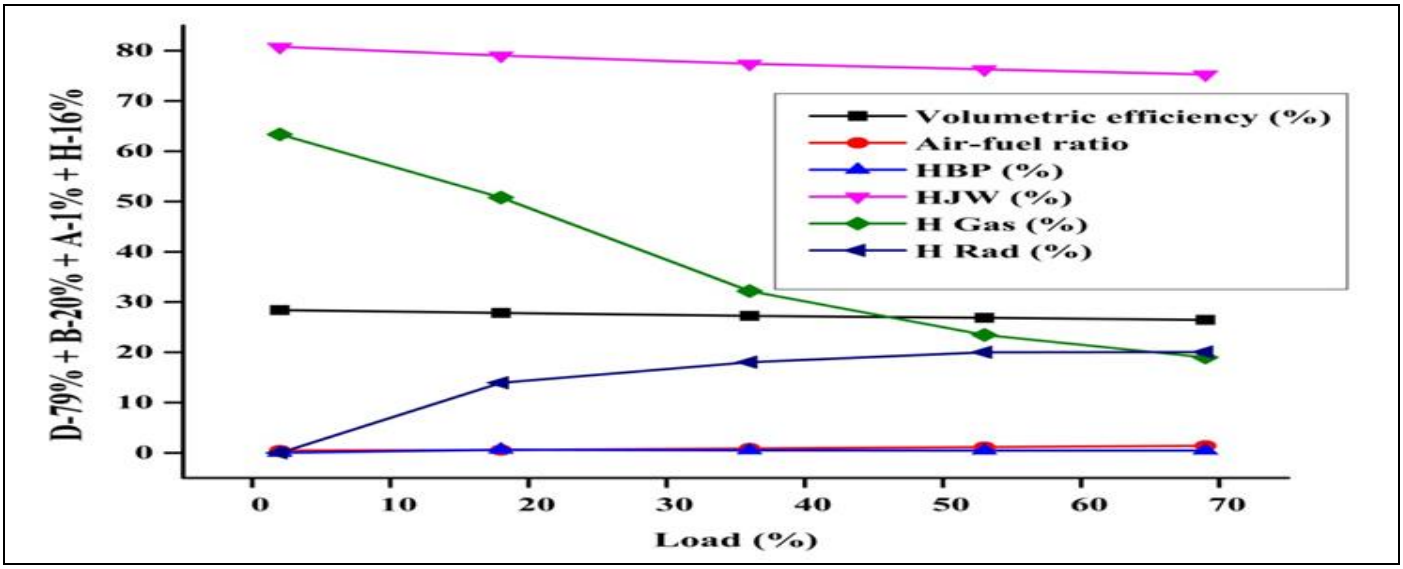

Fig 5 Variation of Compositions of Fuel Versus Loads Percentages.

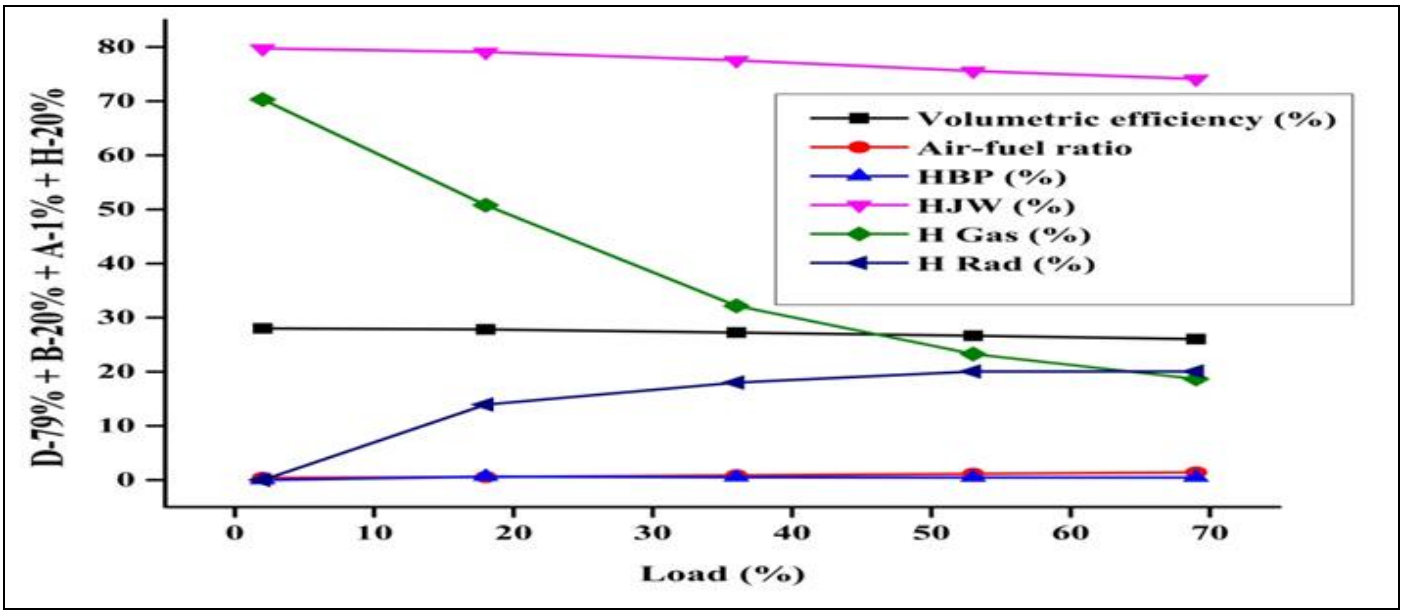

Fig 6 Variation of Compositions of Fuel Versus Loads Percentages.

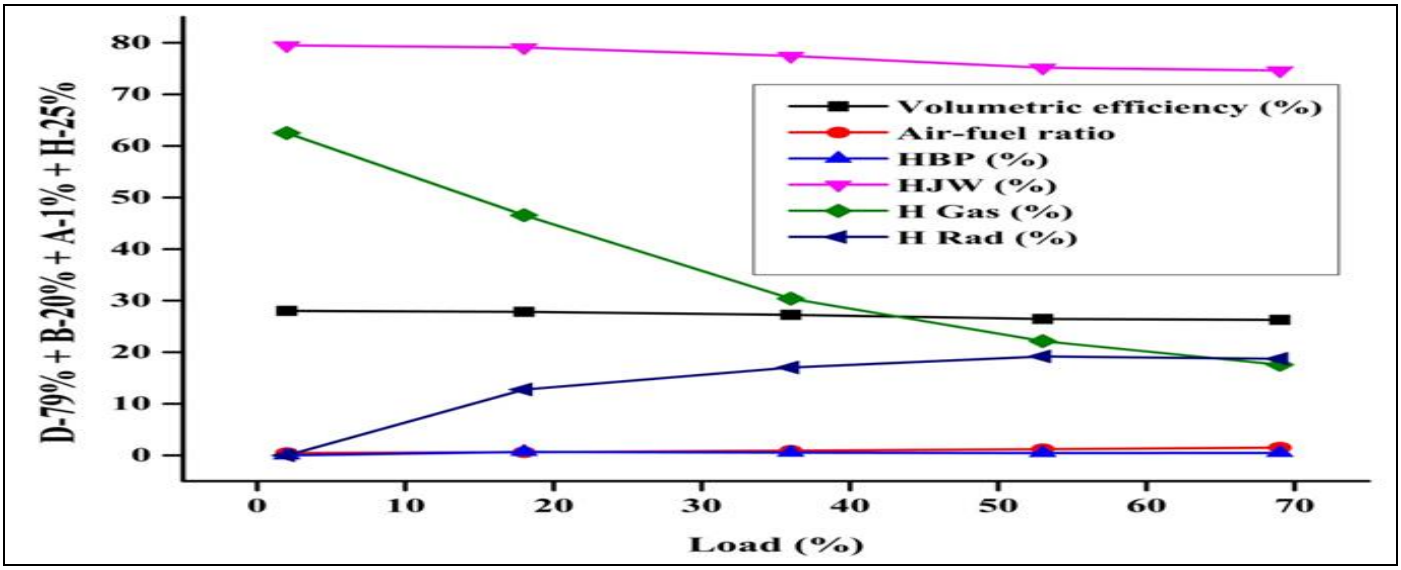

Fig 7 Variation of Compositions of Fuel Versus Loads Percentages.

ISSN No:-2456-2165 https://doi.org/10.5281/zenodo.14608327

In the fuel composition (D-67% + B-30% + A-3% + H-7%), the decrease in volumetric efficiency, heat in jacket water (HJW), heat carried away by exhaust gas (H Gas), and heat carried away by radiation (H Rad) was found to be 3.51%, 3.35%, 13.87%, and 18.32%, respectively. Meanwhile, the air-fuel ratio and heat in brake power (HBP) increased by 10.1% and 18.18%, respectively, compared to the 30% BKO composition at high-load conditions (Fig. 8). In the fuel composition (D-67% + B-30% + A-3% + H-11%), the decreases in volumetric efficiency, HJW, H Gas, and H Rad were 4.23%, 3.87%, 7.97%, and 12.23%, respectively, while the air-fuel ratio and HBP improved by 3.1% and 12.2%, respectively (Fig. 9). Similarly, in the composition (D-67% + B-30% + A-3% + H-16%), the decreases in volumetric efficiency, HJW, H Gas, and H Rad were 5.72%, 5.65%, 15.86%, and 18.2%, respectively, while the air-fuel ratio and HBP increased by 10.1% and 18.18%, respectively (Fig. 10). For the fuel composition (D-67% + B-30% + A-3% + H-20%), the decreases in volumetric efficiency, HJW, H Gas, and H Rad were 6.44%, 6.4%, 16.48%, and 18.2%, respectively, and the air-fuel ratio and HBP improved by 10.07% and 18.18%, respectively (Fig. 11). Finally, in the composition (D-67% + B-30% + A-3% + H-25%), the decreases in volumetric efficiency, HJW, H Gas, and H Rad were 6.44%, 6.46%, 13.4%, and 15.15%, respectively, while the air-fuel ratio and HBP increased by 6.72% and 16.3%, respectively (Fig. 12) (Table 3).

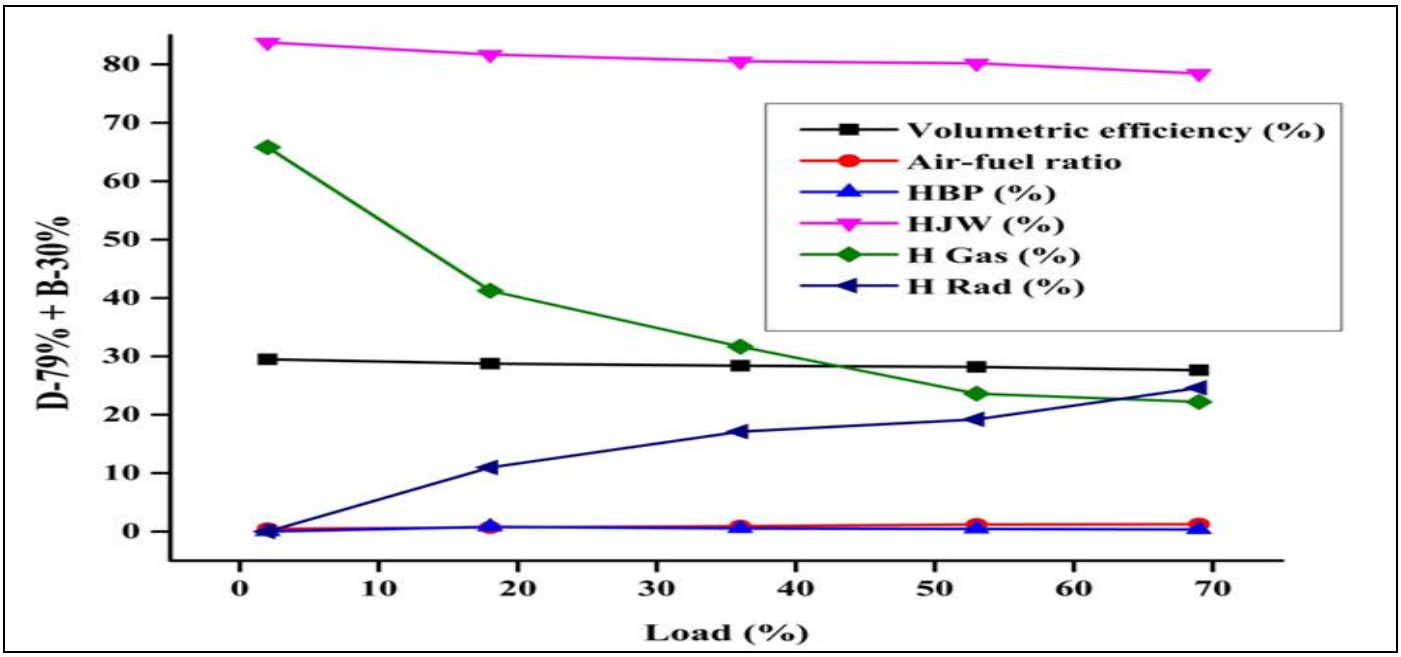

Fig 8 Variation of Compositions of Fuel Versus Loads Percentages.

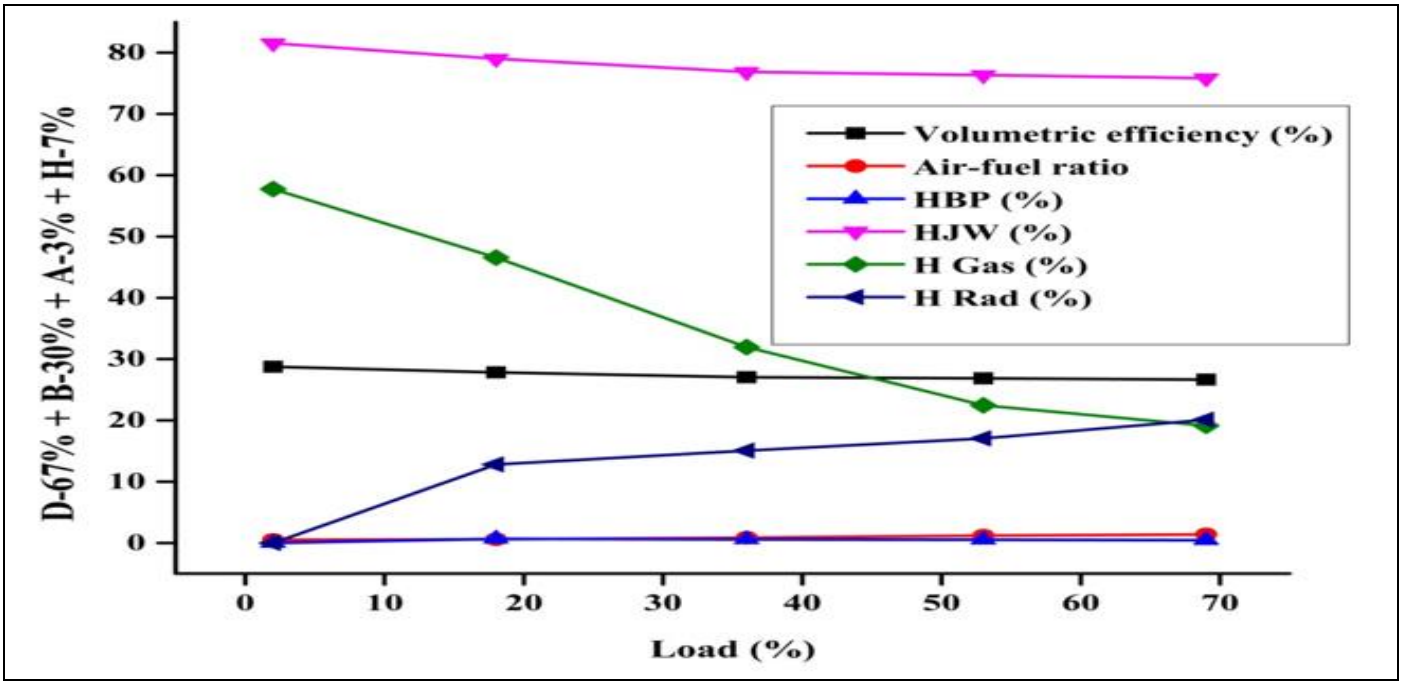

Fig 9 Variation of Compositions of Fuel Versus Loads Percentages.

ISSN No:-2456-2165 https://doi.org/10.5281/zenodo.14608327

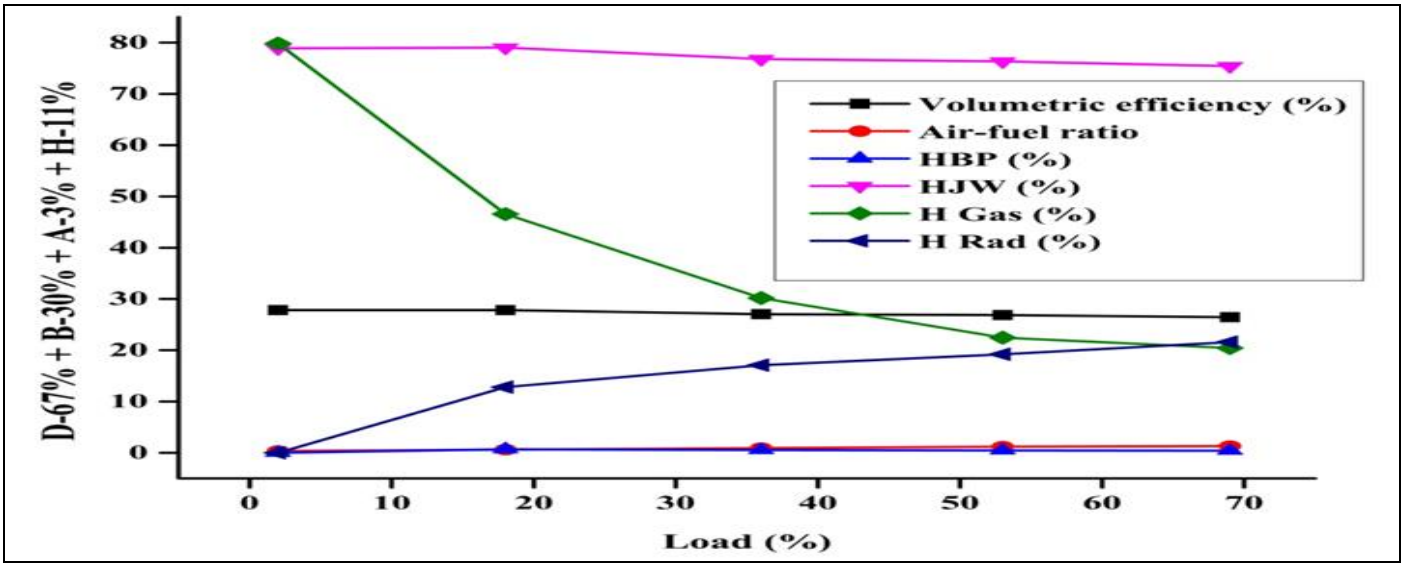

Fig 10 Variation of Compositions of Fuel Versus Loads Percentages.

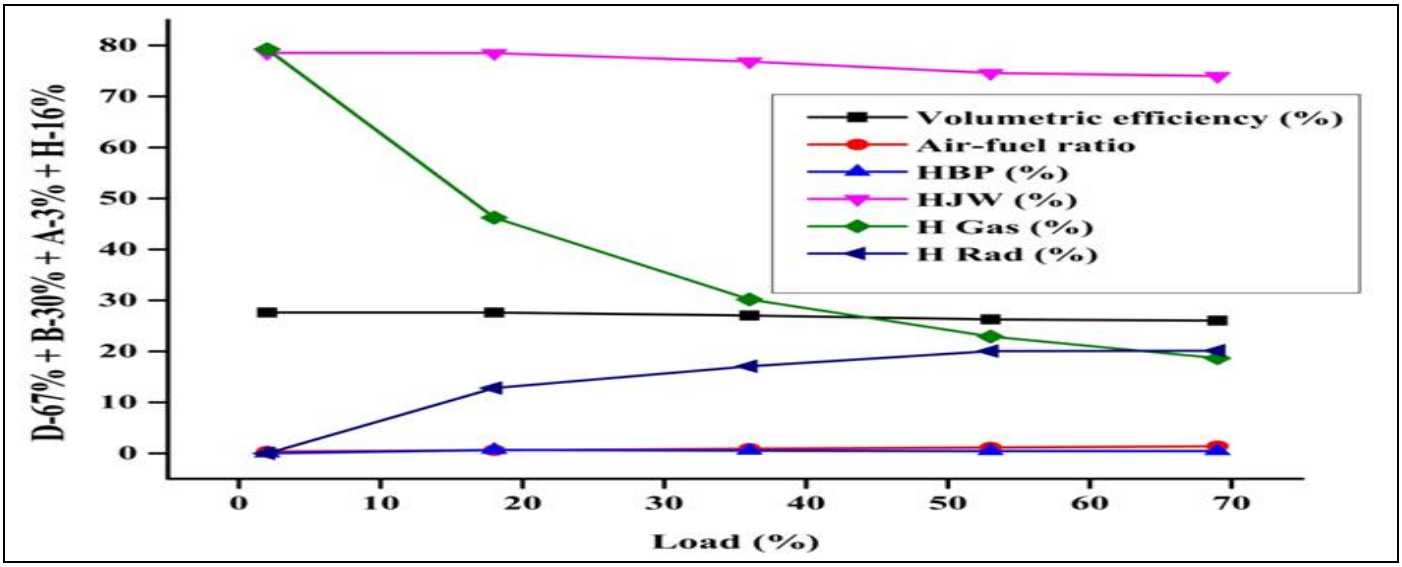

Fig 11 Variation of Compositions of Fuel Versus Loads Percentages.

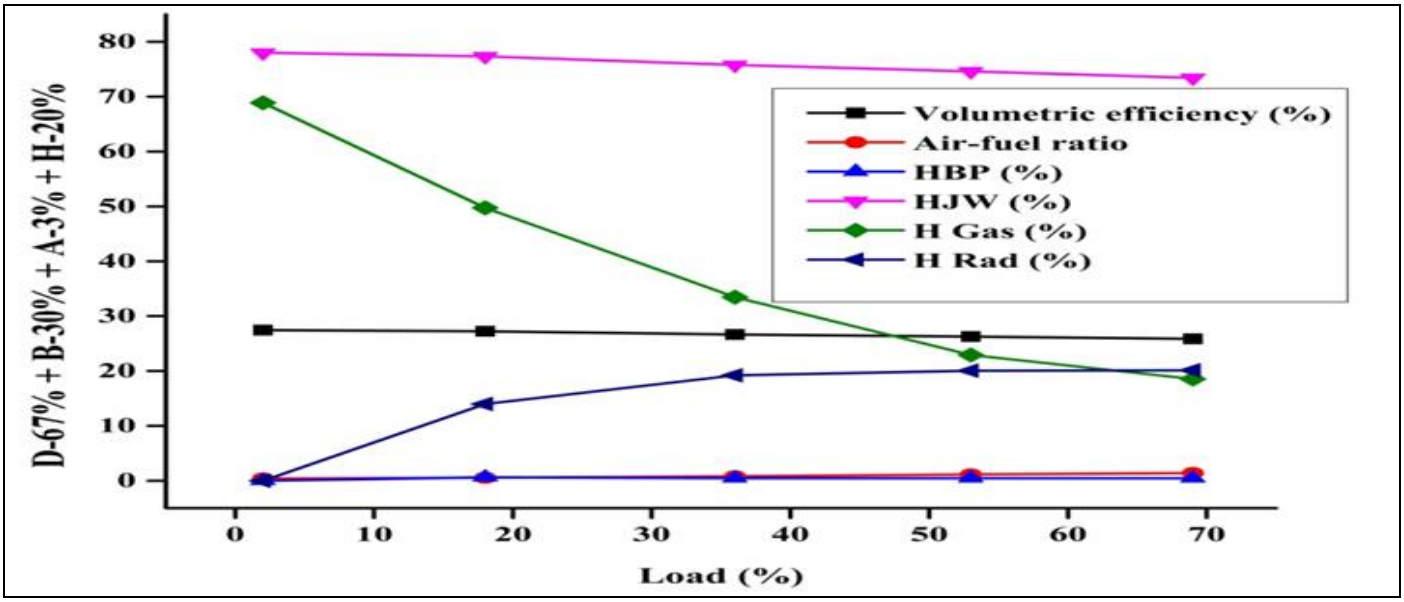

Fig 12 Variation of Compositions of Fuel Versus Loads Percentages.

ISSN No:-2456-2165 https://doi.org/10.5281/zenodo.14608327

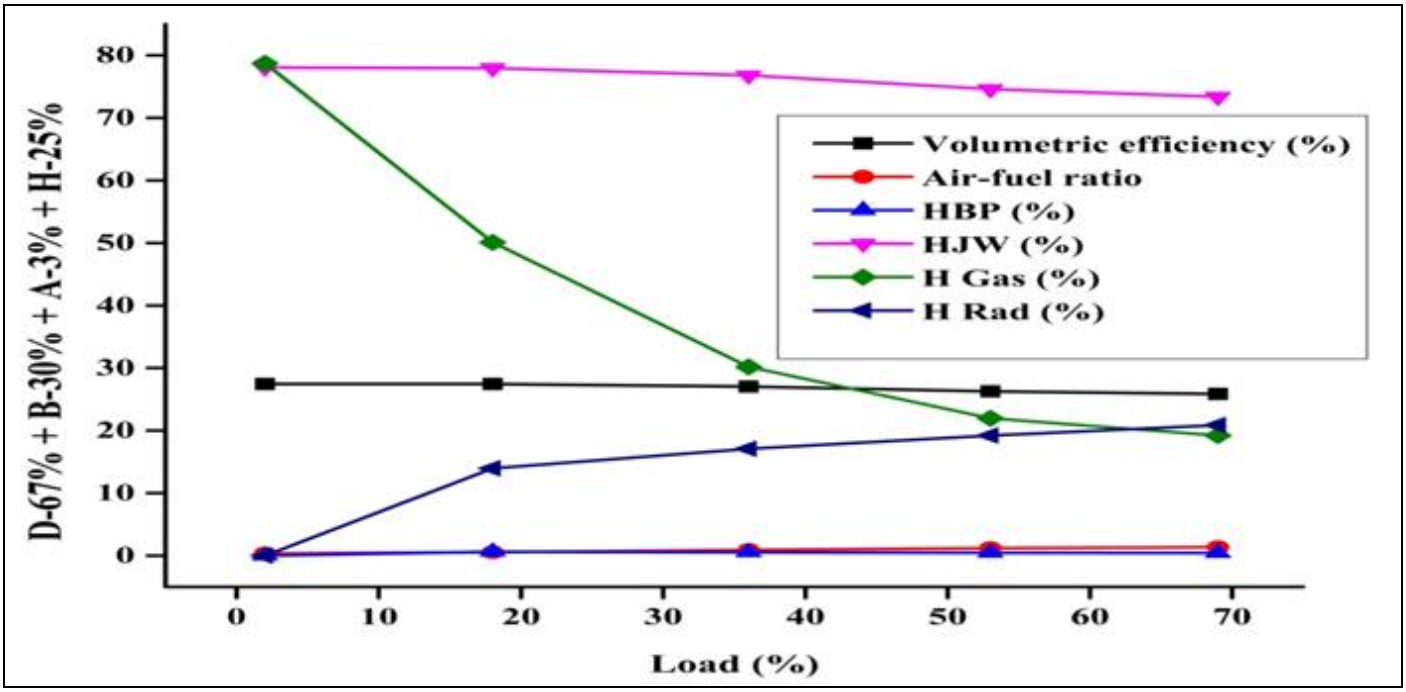

Fig 13 Variation of Compositions of Fuel Versus Loads Percentages.

In the fuel composition (D-55% + B-40% + A-5% + H-7%), decreases in volumetric efficiency, heat in brake power (HBP), heat in jacket water (HJW), and heat carried away by exhaust gas (H Gas) were observed to be 2.67%, 16.27%, 4.54%, and 26.88%, respectively. At the same time, the air-fuel ratio and heat carried away by radiation (H Rad) increased by 14.1% and 18.9%, respectively, compared to the 40% BKO composition under high-load conditions (Fig. 14). For the fuel composition (D-55% + B-40% + A-5% + H-11%), the decreases in volumetric efficiency, HBP, HJW, and H Gas were 4.14%, 0%, 4.19%, and 4.13%, respectively, with no change in the air-fuel ratio and a slight increase of 0.09% in H Rad (Fig. 15). Similarly, for the composition (D-55% + B-40% + A-5% + H-16%), the decreases in volumetric efficiency, air-fuel ratio, HBP, and HJW were 5.53%, 6.7%, 9.3%, and 5.67%, respectively, while H Gas and H Rad increased by 1.97% and 7.49%, respectively (Fig. 16). For the fuel composition (D-55% + B-40% + A-5% + H-20%), the decreases in volumetric efficiency, air-fuel ratio, HBP, HJW, and H Gas were 6.99%, 3.73%, 11.63%, 6.87%, and 3.4%, respectively, while H Rad increased by 11.64% (Fig. 17). Finally, for the fuel composition (D-55% + B-40% + A-5% + H-25%), the decreases in volumetric efficiency, HBP, HJW, and H Gas were 6.99%, 6.97%, 7.12%, and 10.32%, respectively, while the air-fuel ratio and H Rad increased by 3.59% and 5.08%, respectively (Fig. 18) (Table 4).

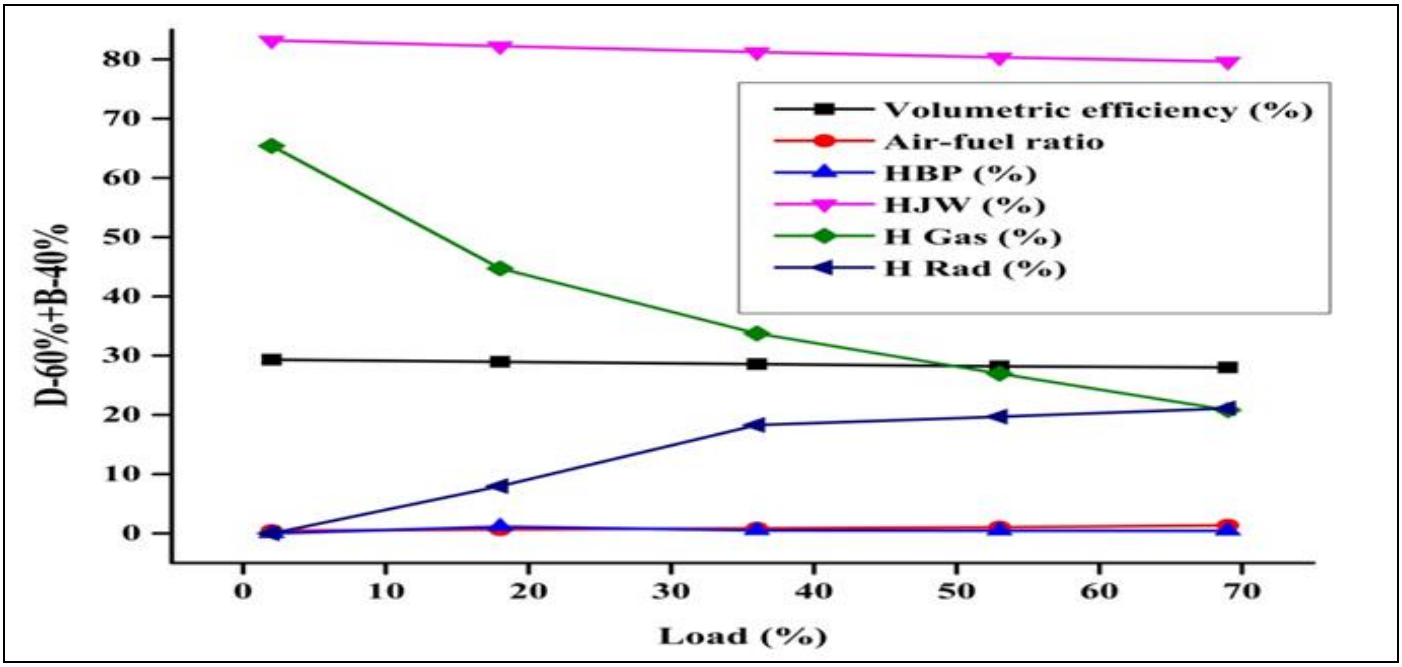

Fig 14 Variation of Compositions of Fuel Versus Loads Percentages.

ISSN No:-2456-2165 https://doi.org/10.5281/zenodo.14608327

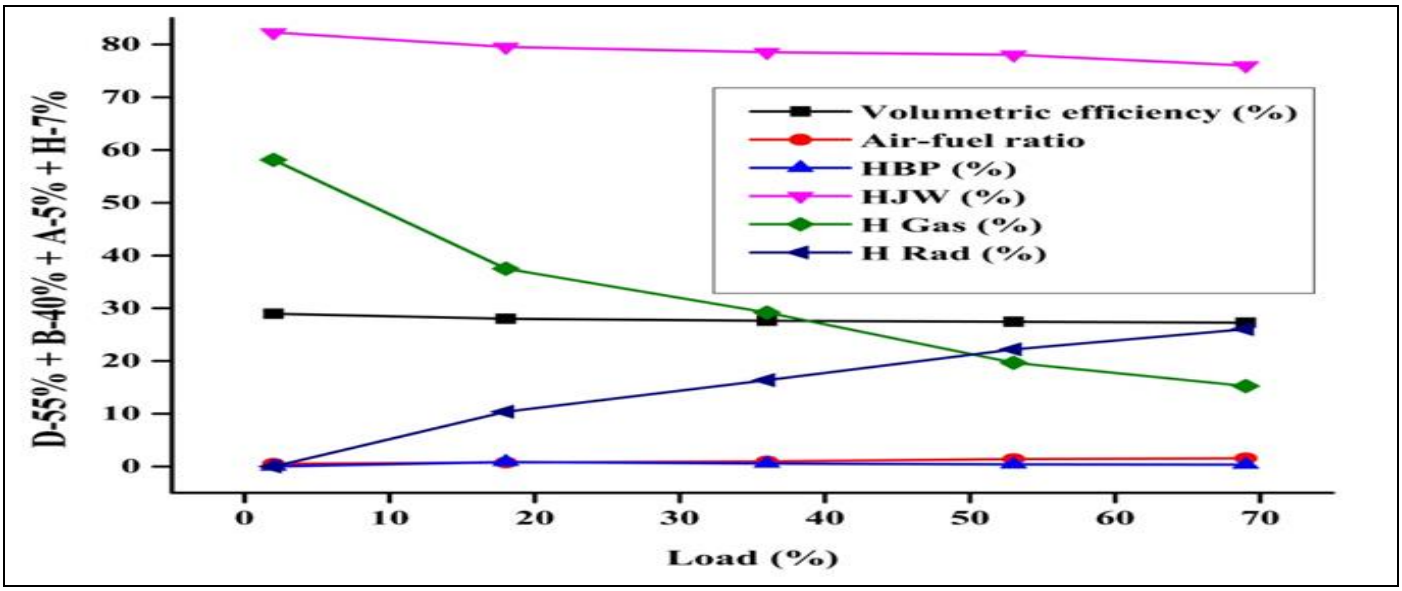

Fig 15 Variation of Compositions of Fuel Versus Loads Percentages.

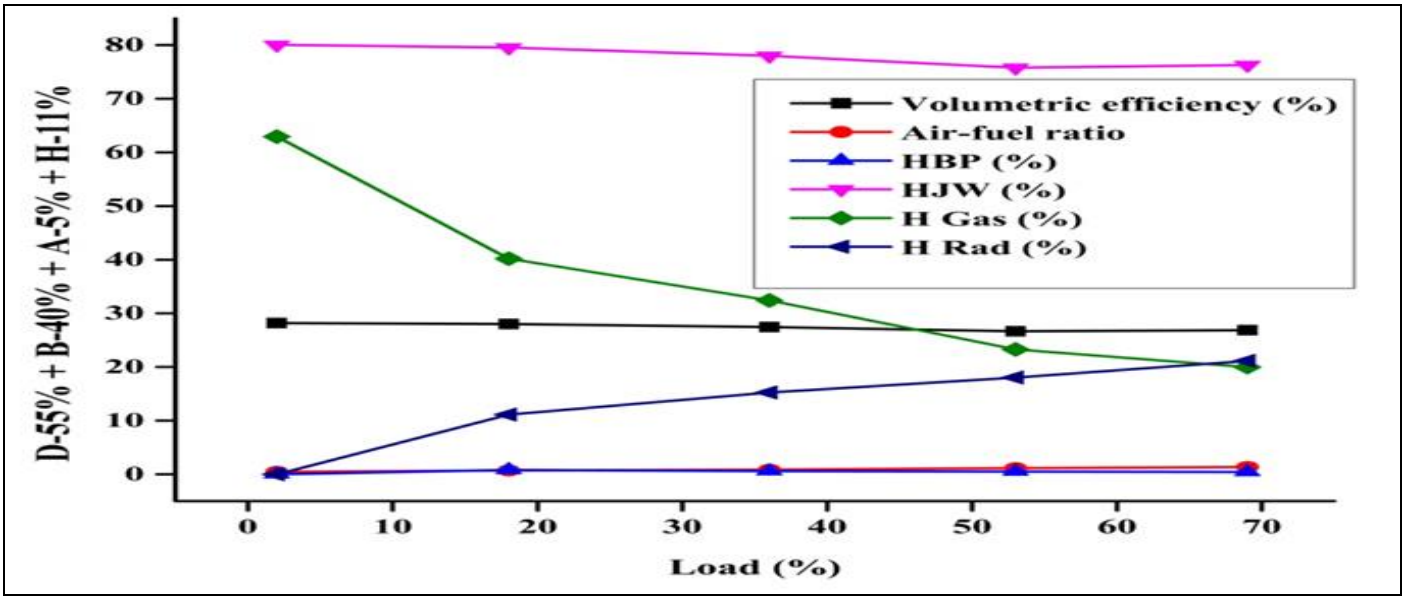

Fig 16 Variation of Compositions of Fuel Versus Loads Percentages.

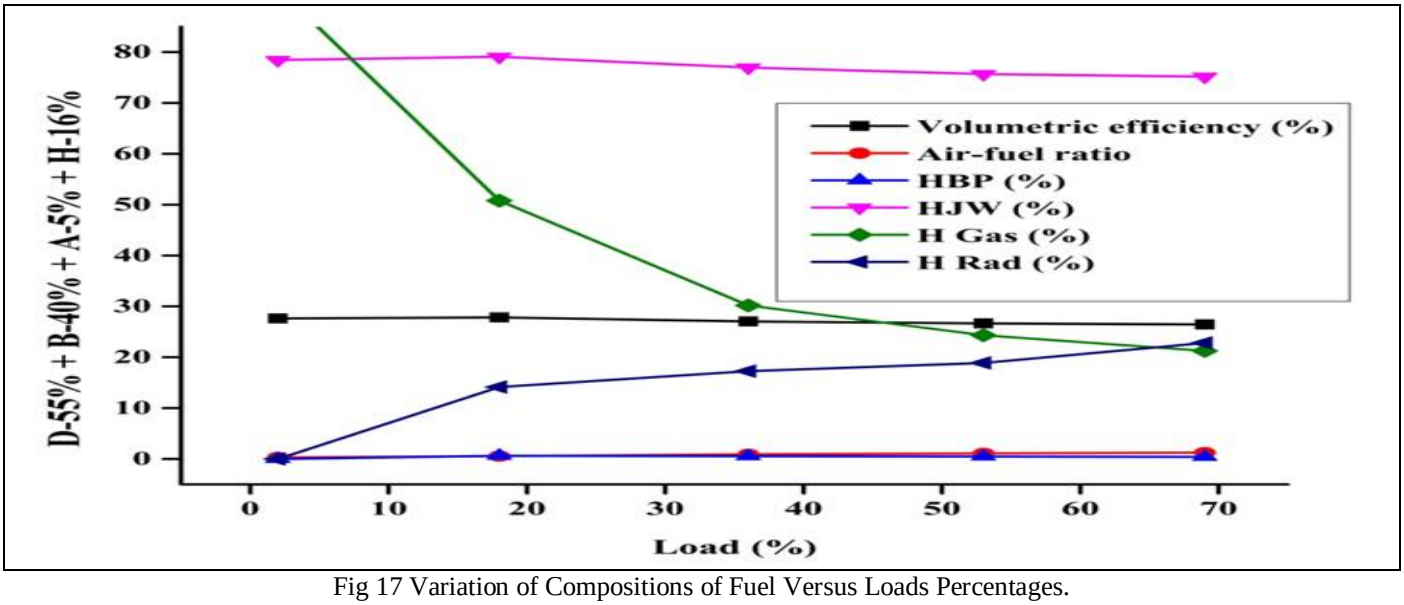

Fig 17 Variation of Compositions of Fuel Versus Loads Percentages.

ISSN No:-2456-2165 https://doi.org/10.5281/zenodo.14608327

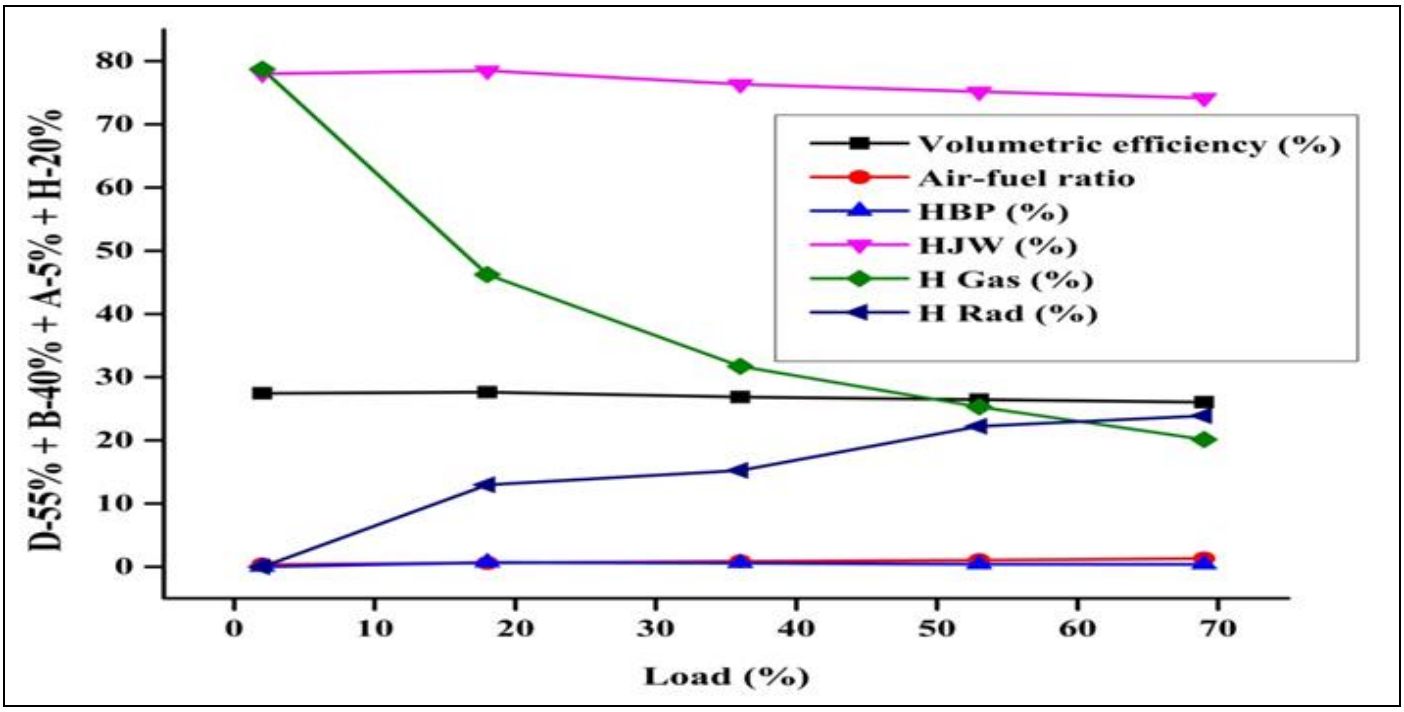

Fig 18 Variation of Compositions of Fuel Versus Loads Percentages.

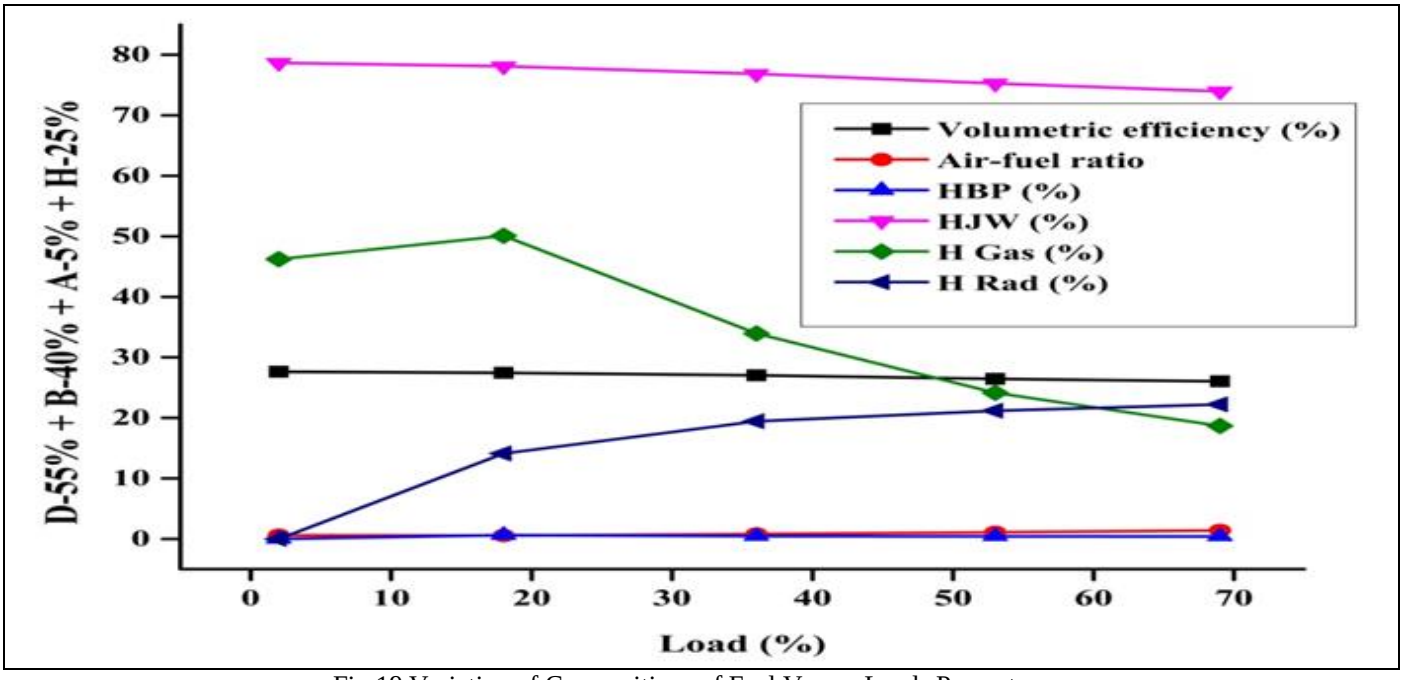

Fig 19 Variation of Compositions of Fuel Versus Loads Percentages.

The engine's volumetric efficiency decreases as the biodiesel content from Karanja oil (BKO) increases from 20% to 40%, the additive increases from 1% to 5%, and the hydrogen content as a secondary fuel increases from 7% to 25% in pure diesel under high-load conditions. This decrease in volumetric efficiency is likely due to the displacement of air by hydrogen, which has a lower density than air, especially as the hydrogen percentage increases.

The air-fuel ratio increases with the addition of BKO from 20% to 30%, the additive from 1% to 5%, and hydrogen from 7% to 25% in each diesel-BKO composition. However, when BKO content reaches 40% in pure diesel with additive and hydrogen, the air-fuel ratio decreases under high-load conditions. This is because hydrogen's lower density compared to air results in less air being used in comparison to diesel-hydrogen mixtures [28].

For heat in brake power (HBP), the value increases with the addition of BKO from 20% to 30%, the additive from 1% to 5%, and hydrogen from 7% to 25% in each diesel-BKO composition at high-load conditions [29]. This increase is due to the gaseous nature of hydrogen, which allows for smoother combustion within the cylinder. However, with a 40% addition of BKO in pure diesel with

ISSN No:-2456-2165 https://doi.org/10.5281/zenodo.14608327

additive and hydrogen, HBP decreases at high-load conditions.

Heat in jacket water (HJW) and heat carried away by exhaust gas (H Gas) decrease with increasing BKO from 20% to 40%, the additive from 1% to 5%, and hydrogen from 7% to 25% in pure diesel under high-load conditions. This reduction is due to the higher thermal conductivity of BKO and hydrogen compared to air in diesel. As a result, less heat is transferred to the jacket water and exhaust gas compared to pure diesel operations [30-31].

Heat carried away by radiation (H Rad) decreases with the addition of BKO from 20% to 30%, the additive from 1% to 5%, and hydrogen from 7% to 25% in each diesel-BKO composition. However, with a 40% addition of BKO in pure diesel with additive and hydrogen, H Rad increases under high-load conditions. This increase is due to the higher mean gas temperature resulting from substituting diesel fuel with hydrogen, which raises the fraction of heat carried away by radiation at higher load conditions [32].

V. CONCLUSIONS

The experiments in this study were conducted on a dual-fuel diesel engine using pure diesel along with various compositions of Karanja oil biodiesel (BKO) (20%, 30%, 40%), an additive (1%, 3%, 5%), and hydrogen (7%, 11%, 16%, 20%, 25%). The parameters examined experimentally included heat carried away by exhaust gas (H Gas), heat carried away by radiation (H Rad), heat in brake power (HBP), heat in jacket water (HJW), air-fuel ratio, and volumetric efficiency. The following findings were observed:

Compared to the fuel composition (D-60% + B-40%), the fuel mixture (D-55% + B-40% + A-5% + H-20%) showed a 6.99% decrease in volumetric efficiency under higher load conditions. The air-fuel ratio decreased by 14.1% when the fuel composition was (D-55% + B-40% + A-5% + H-7%) compared to (D-60% + B-40%) at higher load conditions. The brake power (HBP) was 19.15% higher with the fuel composition (D-79% + B-20% + A-1% + H-25%) compared to (D-80% + B-20%) under higher load conditions. The fuel composition (D-55% + B-40% + A-5% + H-25%) resulted in a 7.12% reduction in heat in jacket water (HJW) compared to (D-60% + B-40%) at higher load conditions. Additionally, the heat carried away by exhaust gas (H Gas) decreased by 26.88% when the fuel composition was (D-55% + B-40% + A-5% + H-7%) compared to (D-60% + B-40%) under higher load conditions. However, the heat carried away by radiation (H Rad) increased by 11.64% when the fuel composition was (D-55% + B-40% + A-5% + H-20%) compared to (D-60% + B-40%) at higher load conditions.

ACKNOWLEDGMENTS

Sunil Mahto would like to acknowledge CSIR-HRDG for providing me with financial support as a fellowship.

REFERENCES

[1]. Thangaraj Suja, Govindan Nagarajan. *Int J Hydrogen Energy* 43 6443 (2018).
[2]. Murugesan A, Umarani C, Subramanian R, Nedunchezhian N. *Renew Sustain Energy Rev* 13 653 (2009).
[3]. Lee CS, Park SW, Kwon SI. *Energy Fuels* 19 2201 (2005).
[4]. Ramanik PK. *Int. J. Renew Energy* 28 239 (2003).
[5]. Baltacioglu M, Arat H, Ozcanli M, Aydin K. *Int J Hydrogen Energy* 41 8347 (2016).
[6]. Banerjee R, Roy S, Bose P. *Int J Hydrogen Energy* 40 12824 (2015).
[7]. Agrawal D, Agrawal AK. *Appl Therm Eng* 27 2314 (2007).
[8]. Sahoo PK, Das LM. *Fuel* 88 1588 (2009).
[9]. Kalam MA, Husnawan M, Masjuki H. *Renew Energy* 2405 (2003).
[10]. Muru gesan A, Umarani C, Subramanian R, Nedunchezhian N . *Renew Sustain Energy Rev* 13 653 (2009).
[11]. Atadashi IM, Aroua MK, Aziz AA. a review. *Renew Sustain Energy Rev* 14 1999 (2020).
[12]. Sharma Abhishek, Murugan S. *Fuel* 108 699 (2013).
[13]. K.A. Abeda, A.K. El Morsi, M.M. Sayed, A.A. El Shaib, M.S. Gad, Egyptian Journal of Petroleum 27 985 (2018).
[14]. Jungkeun Cho , Sangjun Park, Soonho Song. *Energy* 187 115884 (2019).
[15]. Agarwal AK2019), Dhar A. *Automobile Eng* 224 73 (2010).
[16]. Reksowardojo IK, Brodjonegoro TP, Arismunandar W, Sopheak R, Ogawa H. *SAE* pages 1 (2007).
[17]. Forson FK, Oduro EK, Hammond ED. Performance of jatropha oil blends in a diesel engine. *Renew Energy* 29 1135 (2004).
[18]. A.K. Hossain, P.A. Davies, *biomass and bioenergy* 46 332 (2012).
[19]. Jiafeng Sun, Jerald A. Caton, Timothy J. Jacobs *Progress in Energy and Combustion Science* 36 677 (2010).
[20]. H. Raheman, A.G. Phadatare, J R Duling, W Wiyogo and D Debora, *Journal of Physics* 27 393 (2004).
[21]. J R Duling, W Wiyogo and D Debora. *Journal of Physics* Conference Series, 1469 (2018).
[22]. Zhou H, Yi D, Yu Z, Xiao L. J. *Alloys Compds* 438 217 (2007).
[23]. Uzun A, C- evik I˙, Akc-il M. *Surf Coat Technol* 505 116 (1999).
[24]. Parlak A, Yas-ar H, Eldog˘an O. *Energy Convers Manage* 46 489 (2005).
[25]. Abbas Afrasiabi, Mohsen Saremi, Akira Kobayashi *Materials Science and Engineering* A 478 264 (2008).
[26]. Sunil Mahto, Ashish Kumar Saha, Chandra Bhusan Kumar. *International Journal of Hydrogen Energy* 78 938 (2024).
[27]. Sunil Mahto, Satish Saw, Ashish Kumar Saha, Chandra Bhusan Kumar, *International Journal of Hydrogen Energy* 811 363 (2024).

ISSN No:-2456-2165 https://doi.org/10.5281/zenodo.14608327

[28]. Jungkeun Cho, Sangjun Park, Soonho Song, The effects of the air-fuel ratio on a stationary diesel engine under dual-fuel conditions and multi-objective optimization, Energy, Volume 187, 2019, 115884, https://doi.org/10.1016/j.energy.2019.115884.
[29]. H. Raheman, A.G. Phadatare, Diesel engine emissions and performance from blends of karanja methyl ester and diesel, Biomass energy, 27, 2004, 393-397. doi:10.1016/j.biombioe.2004.03.002.
[30]. A.K. Hossain, P.A. Davies, Performance, emission and combustion characteristics of an indirect injection (IDI) multi-cylinder compression ignition (CI) engine operating on neat jatropha and karanj oils preheated by jacket water, Biomass and Bioenergy, Volume 46, 2012, Pages 332-342, https://doi.org/10.1016/j.biombioe.2012.08.007.
[31]. Can Haşimoğlu, Murat Ciniviz, İbrahim Özsert, Yakup İçingür, Adnan Parlak, M. Sahir Salman, Performance characteristics of a low heat rejection diesel engine operating with biodiesel, Renewable Energy, Volume 33, Issue 7, 2008, Pages 1709-1715, https://doi.org/10.1016/j.renene.2007.08.002.
[32]. Can Haşimoğlu, Murat Ciniviz, İbrahim Özsert, Yakup İçingür, Adnan Parlak, M. Sahir Salman, Performance characteristics of a low heat rejection diesel engine operating with biodiesel, Renewable Energy, Volume 33, Issue 7, 2008, Pages 1709-1715, https://doi.org/10.1016/j.renene.2007.08.002.